

Enhanced Raman Scattering of Ultramarine on Au-coated Ge/Si-nanostructures

Elena Klyachkovskaya · Natalia Strekal · Inna Motovich · Svetlana Vaschenko · Anna Harbachova · Mikhail Belkov · Sergey Gaponenko · Christian Dais · Hans Sigg · Toma Stoica · Detlev Grützmacher

Received: 17 September 2010 / Accepted: 16 February 2011 / Published online: 4 March 2011
© Springer Science+Business Media, LLC 2011

Abstract Semiconductor self-assembled Ge-on-Si quantum dot structures coated with Au film were successfully employed as surface-enhanced Raman scattering (SERS) substrates to characterize ultramarine blue inorganic art pigment. To assign the bands and to reveal the enhancement mechanisms, the quantum-chemical calculations of vibration spectra of linear and cyclic model compound of SiO_4 and AlO_4 tetrahedra were carried out. The overtones are observed in the SERS spectra and the unharmonicity constants were estimated. The development of a series of new bands in SERS spectra of ultramarine are discussed in terms of electro-optical unharmonicity.

Keywords Surface-enhanced Raman scattering · Self-organized Ge/Si nanostructures · Au film · Ultramarine · Overtones · Unharmonicity constants

Introduction

The ultramarines are a well-known family of pigments that have been used in artworks for about fifty centuries [1]. In 1828, artificial ultramarine was synthesized by Jean Baptiste Guimet adopted by European artists. Synthetic ultramarine has the approximate formula $\text{Na}_{8-10}\text{Al}_6\text{Si}_6\text{O}_{24}\text{S}_{2-4}$ which can vary with manufacturing conditions, namely purity and proportion of ingredients [2]. The detail structure of natural ultramarines can also vary since it depends on natural deposit. The distinction of natural and synthetic ultramarine is relevant to the analysis of artworks allowing their dating and authenticating.

Raman spectroscopy has become a powerful tool for the purposes of pigments and dyes identification due to the possibility to get valuable information about chemical structure of the objects under investigation. A number of publications have reported on Raman spectroscopy applied to characterize and identify art pigments in canvas and wall paintings [3], historical manuscripts [4], ceramics [5], mosaics [6], and glasses [7].

Ultramarines were also studied by means of Raman spectroscopy [2, 8–11]. However, identification of ultramarine in a number of cases is difficult task for researchers because of surrounding binding media tendency to fluoresce. Moreover, the low concentration of pigment in the paint layers result in weak Raman signals. For these reasons, this tool cannot be applied routinely to identification of pigments in artworks.

The surface-enhanced Raman scattering (SERS) effect significantly enhances the scattering probability when a Raman-active molecule is spatially confined within the electromagnetic field generated upon excitation of the localized surface plasmon resonance (LSPR) in a nano-

E. Klyachkovskaya · S. Vaschenko · A. Harbachova · M. Belkov · S. Gaponenko (✉)
B.I. Stepanov Institute of Physics NASB,
Minsk, Belarus
e-mail: s.gaponenko@ifanbel.bas-net.by

N. Strekal · I. Motovich
Yanka Kupala Grodno State University,
Grodno, Belarus

C. Dais · H. Sigg
Paul Scherrer Institut,
Villigen, Switzerland

T. Stoica · D. Grützmacher
Institute of Bio- And Nanosystems,
Jülich, Germany

textured surface of a noble metal [12]. The increases in the intensity of Raman signal have been regularly observed on the order of 10^4 – 10^6 , and can be as high as 10^{14} in certain portions of space (so called “hot spots”) for certain systems [13–15]. Enhancement of Raman scattering occurs owing to the three distinct mechanisms [16]. The primary one is high spatial concentration of incident field resulting in more efficient excitation of a probe molecule. This mechanism is identical to simple increase in incident light intensity. Enhancement then equally occurs for all originally existing Raman lines. The second one is spectral redistribution of electromagnetic mode density (photon density of states). Because of frequency dependence of mode density enhancement, this mechanism acts differently at different Raman lines but it cannot promote development of new lines. Finally, the third mechanism can result in development of new lines in Raman spectra resulting from newly arising chemical bonds as well as anharmonism of molecular vibrations.

Because of high-enhancement factors, the samples required for SERS could be microscopic in size, of the order of a few powder grains or crystallites, which can be safely taken from delicate pieces leaving no visible damage on the objects. Recently, a number of papers have reported successful application of SERS to identify highly fluorescent organic dyes and lake pigments [17–22]. In addition to direct enhancement of Raman signal, nanotextured noble metal substrates offer drastic quenching of otherwise competitive or even dominating fluorescence thus increasing Raman-based detectability of pigments [23–25]. In the recent years, several noble metal nanostructures have been proposed as SERS active substrates [26–29].

In the present paper, the Au-coated semiconductor self-assembled quantum dot Ge-on-Si nanostructures are shown to enhance considerably Raman signal of inorganic art pigment known as ultramarine blue and the enhancement mechanism are discussed.

Experimental

SERS substrates were prepared by vacuum deposition of Au on top of the semiconductor self-assembled quantum dot Ge-on-Si structures which were grown by chemical vapor deposition. After in situ annealing at 900 °C, the growth was performed at 680–700 °C using SiH₂Cl₂ and GeH₄ as reactive gasses in an H₂ atmosphere at $p_{\text{tot}}=0.1$ Torr [30]. The sequence of deposited layers is following: Si-substrate/12 nm Si/7ML Ge/40 nm Si capping layer.

In Fig. 1, the AFM surface scans from a SERS substrate (#2058) are present. The sample surface consists of germanium pyramids with a square base randomly distributed on silicon substrate (Fig. 1).

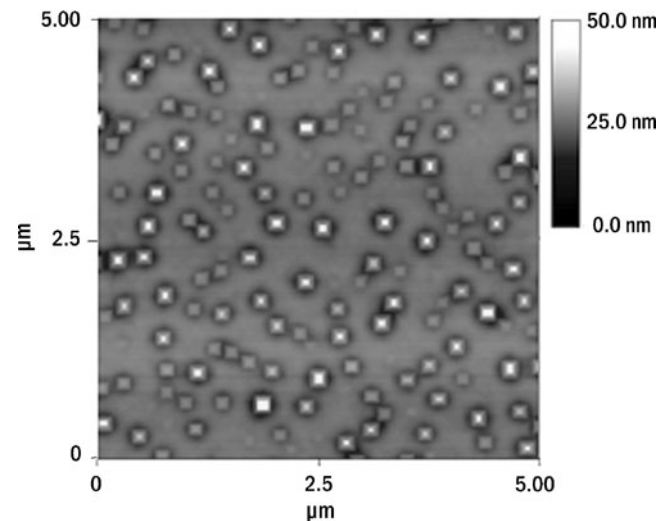


Fig. 1 AFM images of the substrate surface with pyramid-shape islets on the top of Ge-on-Si substrate

The ultramarine suspension that was prepared using ultrasonic disperser has been deposited on the SERS substrate and dried at room temperature in the horizontal position. Ultramarine suspension by the same manner was also deposited on the reference Au-free Ge-on-Si substrate. To record the Raman spectrum of the ultramarine, the powder of the pigment (that we will use as reference) has been put in capillary.

The Raman measurements were performed in the backscattering configuration at room temperature on a Spectra Pro-500i spectrometer (Acton Research, USA) using the second harmonic radiation of a cw diode-pumped Nd-YAG-laser, the excitation wavelength was 532 nm. A holographic filter, a diffraction grating (600 lines/mm), and a cooled Si CCD detector were used for Raman spectra recording. Reflection and transmission spectra were measured with a commercial UV-visible spectrophotometer Carry-500 (Varian, USA).

Results and Discussion

The reflection spectrum of the SERS substrate with evaporated gold film and the absorption spectrum of ultramarine suspension are presented in Fig. 2. The bath with deionized water was put in reference channel when measuring optical transmission for ultramarine suspension. The LSPR maximum in reflection spectrum of the substrate and the absorption bands of ultramarine suspension overlap. That is the precondition to detect surface-enhanced Raman scattering of ultramarine.

The Raman spectrum of ultramarine powder is presented in Fig. 3a. In the spectrum the symmetric stretching vibration ν_1 of S₃⁺ at 541 cm⁻¹ and the bending vibration

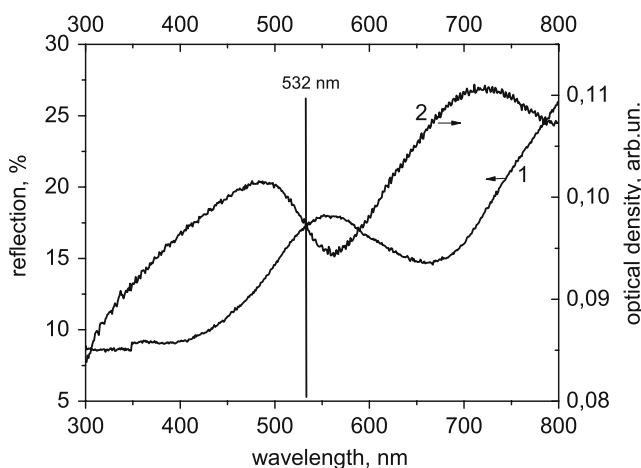


Fig. 2 1 The reflection spectrum of the Au-coated Ge/Si substrate #2058-24 (IBN-1, Julich) and 2 optical density spectrum of water suspension of ultramarine blue #45010 (Kremer, Aichstetten)

ν_2 of S_3^- at 258 cm^{-1} are seen. In addition, the overtones of the stretching vibration $2\nu_1$ and $3\nu_1$ at $1,093$ and $1,641\text{ cm}^{-1}$, respectively, are also visible.

The Raman spectrum of the ultramarine suspension on the top of the reference Ge-on-Si substrate is shown in Fig. 3b. All bands of strong and medium intensities in the spectrum correspond to characteristic Raman bands of the pure Ge-on-Si substrate [31, 32]. Namely, the peak at 517 cm^{-1} can be assigned to the Si-Si bond, and the peaks at 292 and 409 cm^{-1} can correspond to Ge-Ge and Ge-Si vibrations, respectively. The stretching and bending vibrations of S_3^- inherent in ultramarine have so weak intensities that their occurrence in the spectrum is questionable.

The Raman spectrum detected with Au-coated Ge-on-Si substrate is presented in Fig. 3c. Drastic increasing of the

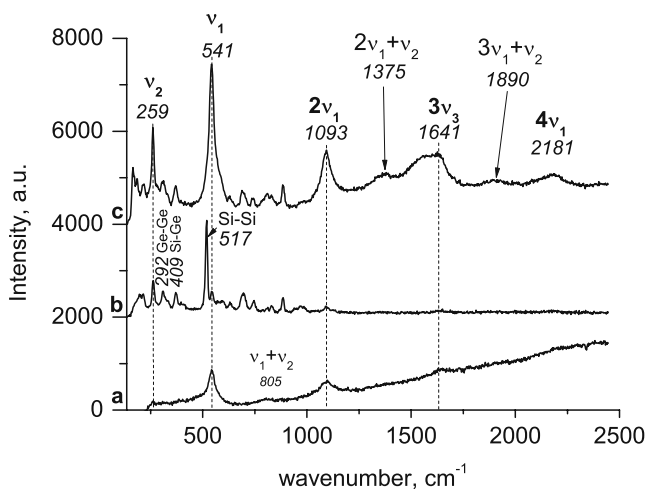


Fig. 3 Raman spectrum of ultramarine blue pigment **a** in powder, **b** in aqueous suspension deposited on top of a reference Au-free Si-on-Ge substrate, and **c** on the Au-coated Si-on-Ge substrate

ultramarine characteristic bands intensities in the spectrum is evident. It is accompanied with the occurrence of some new narrow bands in the spectral range 200 – $1,000\text{ cm}^{-1}$ and a series of wide bands in spectral range $1,000$ – $2,500\text{ cm}^{-1}$. The latter by their position and shape can be assigned to a series of overtones and combination modes. Taking into account that detection of stretching and bending vibration of S_3^- in the Raman spectrum of the ultramarine suspension deposited on the reference substrate was questionable, it is reasonable to conclude on considerable enhancement of Raman signals provided by a Au-coated Ge-on-Si substrate. The average enhancement per ensemble of ultramarine crystallites deposited over the substrate is at least tenfold for every line except that at 541 cm^{-1} .

According to our calculations for silver spherical particles [33], enhancement rapidly falls down from 10^{10} at 0.1 nm distance to 10 for 40 nm distance in the case of normal orientation of the dipole moment of a molecule and down from 10^6 at 0.1 nm to 1 for 40 nm in the case of tangential orientation of the dipole moment of a molecule. In our experiments, we did not take care about the orientation of the dipole moment of the ultramarine crystals that result in decreasing of the maximum value of enhancement. Further, the size of ultramarine particles even after ultrasonic dispersion is at the average $1\text{ }\mu\text{m}$. Therefore we consider that 40 nm are 10% of average size approx (or even less), i.e., only 0.001 volume fraction contributes to Raman signal enhancement. Taking into account that surface coverage of pyramids is approximately 10% , we have that 0.001 portion of crystallites' volume distributed over the surface with 0.1 probability to fall into close proximity to pyramids showed tenfold enhancement. Then average enhancement within this 0.001 portion of crystallites' volume have enhancement factor of 10^5 while local enhancement can monotonously fall down from higher values to 1 within that portion.

It should be noted that the bands assignment in the Raman spectra of ultramarines is different in the works of different authors. For example, one group of authors assign the bands at 260 and 540 cm^{-1} to fundamental vibrations of S_3^- and the band at $1,093\text{ cm}^{-1}$ to the first overtone of the stretching vibration of S_3^- [8]. At the same time, the other authors [33] assign these bands to vibrations of aluminosilicate framework. The problem of the bands assignment in the observed SERS spectrum is of principal importance in the context of evaluation of enhancement mechanisms. Namely, the electromagnetic enhancement mechanism of Raman scattering implies, first of all, enhanced excitation efficiency by means of the incident electromagnetic field concentration [13]. This mechanism cannot result neither in development of new bands nor in relative intensity changes of originally existing bands. Second,

density of states effect can contribute to Raman scattering enhancement [15, 34] and in this case the relative change in the intrinsic bands intensity may arise because of spectral distribution of density of states. However, the new bands cannot develop. Third, chemical mechanisms can contribute and in this case the new, originally not presented, bands can develop in the SERS spectrum. Therefore, modeling of vibrations in ultramarine has been performed with the aim to assign the new Raman bands in SERS spectrum of ultramarine to aluminosilicate framework. We assume that these atom groups may be found in close contact with gold surface and experience the effect of enhancement in first layer.

The framework of the sodalite type is based on the β cages, which are built from SiO_4 and AlO_4 tetrahedra (Fig. 4). Three Na^+ ions locate inside each cavity to neutralize the deficit in positive charges introduced by the presence of aluminum instead of silicon in the framework. In addition to these Na^+ ions, a salt can be encapsulated in the β cages [1].

The quantum-chemical calculations of characteristic vibration modes for SiO_4 and AlO_4 units were performed for model compounds, which optimized geometry is presented in Fig. 5. These are the linear “diatomic” (Fig. 5a) and cyclic quadruple (Fig. 5b) systems assembled of SiO_4 and AlO_4 tetrahedra. All the calculated and observed modes in the normal Raman and SERS spectra are presented in Table 1.

The calculations show that vibrations of aluminosilicate framework can really appear in the spectral range of 200–1,000 cm^{-1} . This range is the range of characteristic vibrations for both the framework and chromophore atoms. It is important that stretching vibrations of the framework are antisymmetric and must have high activity in IR

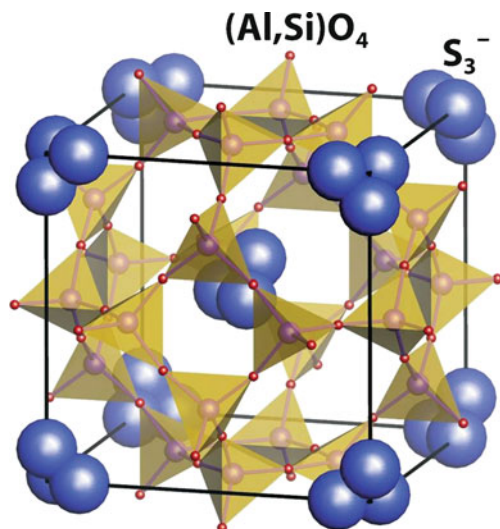


Fig. 4 Crystal cell of ultramarine

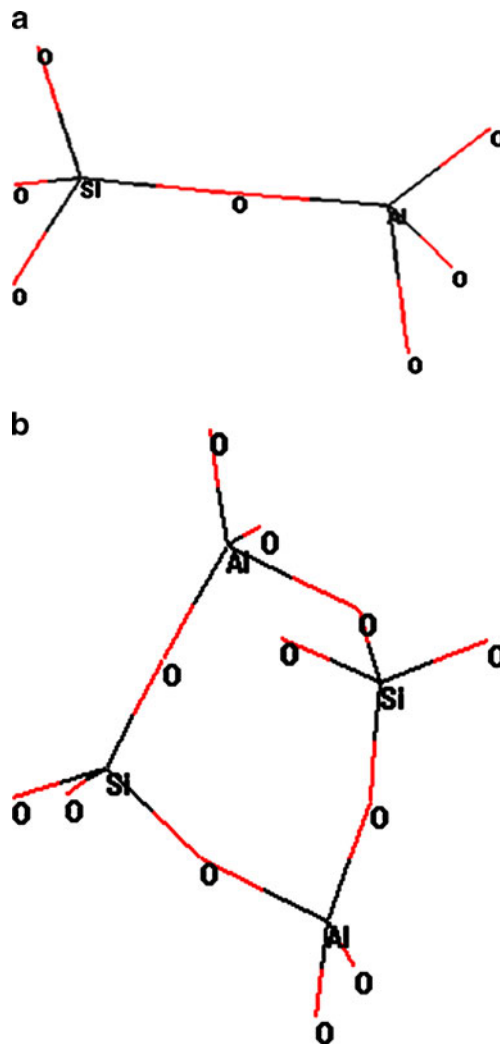


Fig. 5 The model of linear (a) and quadruple (b) bonds of SiO_4 and AlO_4 tetrahedra

absorption. The possible development of such a vibration bands in SERS may be caused by specific “surface rules”, i.e., reduction of symmetry due to chemical mechanism of enhancement.

One can see ultramarine features pronounced environment influence on the anharmonicity of vibration. Earlier, the observation of overtones and combinations in the SERS spectra of single molecule dispersed in Langmuir–Blodgett monolayers is confirmed for a family of molecules—perylene-tetracarboxylic diimides [35]. Overtone and combination progressions are well resolved in [35] and correspond to equidistant vibrational levels. Any presumption about vibration anharmonicity responsible for the development of overtones and combinations are absent in discussed paper.

In contrast, in the case of ultramarine, it is clearly seen that the overtones and combinations have appeared in SERS due to vibration anharmonicity, because the over-

Table 1 Wave numbers (cm^{-1}) of vibration bands in the standard Raman and SERS spectra (this work), calculated data for the model compounds (Fig. 5) and reference data for the S_3^- chromophore

| Ultramarine | | SiAlO ₇ (Fig. 5a) | | Si ₂ Al ₂ O ₁₂ (Fig. 5b) | | S_3^- | | |
|----------------------|------------|------------------------------|-----------------------------------|---|--|------------|-------------------|------|
| Standard Raman lines | SERS lines | Calculated Raman lines | Assignment | Calculated Raman lines | Assignment | Raman line | Assignment | Ref. |
| 259 | 259 | 242 | $\delta(\text{SiOAl})$ | 262 | $\delta(\text{SiOAl}), \delta(\text{OAlO}),$ | 258 | δS_3^- | [2] |
| 541 | 541 | | | 533 | Ring breathing | 548 | $\nu_1 S_3^-$ | [2] |
| | 795 | 803 | $\nu(\text{OSiO})$ antisymmetric | 809 | $\nu(\text{OSiO})$ antisymmetric | | | |
| | | | | 1080 | $\nu(\text{SiOAl})$ antisymmetric, $\nu(\text{OAlO})$ antisymmetric | | | |
| 1098,7 | 1091 | 1109 | $\nu(\text{SiOAl})$ antisymmetric | 1105 | $\nu(\text{SiOAl})$ antisymmetric, $\nu(\text{OAlO})$ antisymmetric | 1096 | $2\nu_1 S_3^-$ | [2] |
| | 1364 | | | | | | $2\nu_1 + \delta$ | |
| | 1639 | | | | | 1644 | $3\nu_1 S_3^-$ | [2] |
| | 1905,4 | | | | | | $3\nu_1 + \delta$ | |
| | 2186,1 | | | | | 2195 | $4\nu_1 S_3^-$ | [2] |

tones sequence is not equidistant (as in the case of Raman spectra [2]), but is divergent.

The expression for vibration terms is following: (in cm^{-1})

$$E_v = v(v + 1/2) - vx_e(v + 1/2)^2 + vy_e(v + 1/2)^3 - \dots, \quad (1)$$

where, x_e is the mechanical unharmonicity constant and y_e is the electro-optical one.

The expression for vibration energy turns into $E_v = v(v + 1/2)$ if $x_e \approx 0$ and $y_e \approx 0$ and the harmonic vibrations (with equidistant vibration level/band sequence) are observed.

The mechanical vibrational unharmonicity appears when $x_e \neq 0$, the series of overtones are occurring and the vibration level/band sequence became converging. The third component in the expression (1) can give the contribution in the case of considerable electro-optical unharmonicity. In this case, the divergent sequence of vibrational bands must develop.

Our estimation gives the following values for the unharmonicity constants and the fundamental vibration mode: $x_e = 0,0034$, $y_e = 0,0011$, and $\nu_1 = 544,35 \text{ cm}^{-1}$. This estimation also shows that the light divergence of overtones bands can be explained if assumption that both mechanical force and induced dipole moment, and hence, polarizability of ultramarine have a nonlinear vibration coordinates dependence on the top of plasmon surface.

According to available data, the appearance of overtone and combination modes of fundamental vibrations bands of ultramarine in SERS spectra is observed for the first time. The relatively high value of electro-optical unharmonicity constants is indicative of strong chemical enhancement mechanism of SERS.

Conclusion

The vacuum deposition of gold on the surface of semiconductor self-assembled Ge-on-Si quantum dot structures allow to detect SERS spectra of ultramarine blue inorganic art pigment. In SERS spectra of ultramarine, the series of narrow bands in the spectral range 200–1,000 cm^{-1} and a series of wide bands in spectral range 1,000–2,500 cm^{-1} are developed. These narrow bands may be assigned to ultramarine framework vibrations in the close vicinity to gold surface, because the characteristic vibration bands of aluminosilicate groups lie in this range as it follows from the calculations performed. The wide bands in high-frequency range are assigned to overtones and combinations of S_3^- fundamental modes. For the first time, the relatively high value of electro-optical vibrational unharmonicity is estimated for the SERS spectra of ultramarine and the principal measurability of such a constant near the SERS-active gold surface has high importance for the chemical mechanism of SERS enhancement elucidation. The observed enhancement factors are different for different bands ranging from approximately one order of the magnitude for the principal bands to two orders of the magnitude for overtones and linear combinations of principal modes. The results demonstrate feasibility of more sensitive detection of ultramarine by means of Au-coated Ge-on-Si nanostructures and can be purposefully used in cultural heritage examination.

Acknowledgment Helpful discussions with K. Kneipp and D. Guzatov are greatly acknowledged. The work has been supported Belarusian National Program “Crystalline and Molecular Structures” and Swiss Program “SCOPE”.

References

1. Seel F (1984) Sulphur in artwork: lapis lazuli and ultramarine pigments. *Stud Inorg Chem* 5:67–89
2. Osticioli I, Mendesa NFC, Nevinc A, Gil FPSC, Becuccia M, Castellucci E (2009) Analysis of natural and artificial ultramarine blue pigments using laser induced breakdown and pulsed Raman spectroscopy, statistical analysis and light microscopy. *Spectrochim Acta A* 73(3):525–531
3. Burratato G, Calabrese M, Cosentino A, Gueli AM, Troja SO, Zuccarello A (2004) ColoRaman project: Raman and fluorescence spectroscopy of oil, tempera and fresco paint pigments. *J Raman Spectrosc* 35(10):879–886
4. Clark RJH, van der Weet J (2004) Identification of pigments and gemstones on the Tours Gospel: the early 9th century Carolingian palette. *J Raman Spectrosc* 35(4):279–283
5. Striova J, Lofrumento C, Zoppi A, Castellucci M (2006) Prehistoric Anasazi ceramics studied by micro-Raman spectroscopy. *J Raman Spectrosc* 37(10):1139–1145
6. Galli S, Mastelloni M, Ponterio R, Triscari M (2004) Raman and scanning electron microscopy and energy-dispersive x-ray techniques for the characterization of colouring and opaquening agents in Roman mosaic glass tesserae. *J Raman Spectrosc* 35(8–9):622–627
7. Welter N, Schüssler U, Kiefer W (2007) Characterisation of inorganic pigments in ancient glass beads by means of Raman microspectroscopy, microprobe analysis and X-ray diffractometry. *J Raman Spectrosc* 38(1):113–121
8. Clark RJH, Franks ML (1975) The resonance Raman spectrum of ultramarine blue. *Chem Phys Lett* 34(1):69–72
9. Gobeltz N, Demortier A, Lelieur JP, Duhayon C (1998) Correlation between EPR, Raman and colorimetric characteristics of the blue ultramarine pigments. *J Chem Soc Faraday Trans* 94(5):677–681
10. Bacci M, Cucci C, Federico ED, Ienco A, Jerschow A, Newman JM, Picollo M (2009) An integrated spectroscopic approach for the identification of what distinguishes Afghan lapis lazuli from others. *Vib Spectrosc* 49(1):80–83
11. Schmidt CM, Walton MS, Trentelman K (2009) Characterization of lapis lazuli pigments using a multitechnique analytical approach: implications for identification and geological provenance. *Anal Chem* 81(20):8513–8518
12. Haynes CL, Van Duyne RP (2001) Nanosphere lithography: a versatile nanofabrication tool for studies of size-dependent nanoparticle optics. *J Phys Chem B* 105(24):5599–5611
13. Kneipp K, Moskovits M, Kneipp H (2006) Surface-enhanced Raman scattering. Springer, Berlin
14. Kneipp K, Kneipp H, Itzkan I, Dasari RR, Feld MS (1999) Ultrasensitive chemical analysis by Raman spectroscopy. *Chem Rev* 99:2957–2975
15. Gaponenko SV, Guzatov DV (2009) Possible rationale for ultimate enhancement factor in single molecule Raman spectroscopy. *Chem Phys Lett* 477(4–6):411–414
16. Gaponenko SV (2010) Introduction to nanophotonics. Cambridge University Press, Cambridge
17. Leona M, Lombardi JR (2007) Identification of berberine in ancient and historical textiles by surface-enhanced Raman scattering. *J Raman Spectrosc* 38(7):853–858
18. Chen K, Leona M, Vo-Dinh T (2007) Surface-enhanced Raman scattering for identification of organic pigments and dyes in works of art and cultural heritage material. *Sens Rev* 27(2):109–120
19. Leona M, Stenger J, Ferloni E (2006) Application of surface-enhanced Raman scattering techniques to the ultrasensitive identification of natural dyes in works of art. *J Raman Spectrosc* 37(10):981–992
20. Lau D, Livett M, Prawer S (2008) Application of surface-enhanced Raman spectroscopy (SERS) to the analysis of natural resins in artworks. *J Raman Spectrosc* 39(4):545–552
21. Whitney AV, Casadio F, Van Duyne RP (2007) Identification and characterization of artists' red dyes and their mixtures by surface-enhanced Raman spectroscopy. *Appl Spectrosc* 61(9):994–1000
22. Brosseau CL, Rayner KS, Casadio F, Crzywacz CM, Van Duyne RP (2009) Surface-enhanced Raman spectroscopy: a direct method to identify colorants in various artist media. *Anal Chem* 81(17):7443–7447
23. Jeannaire DL, Van Duyne RP (1977) Surface Raman spectroelectrochemistry. Part 1. Heterocyclic, aromatic, and aliphatic amines adsorbed on the anodized silver electrode. *J Electroanal Chem* 81:1–20
24. Albrecht MA, Creighton JA (1977) Anomalously intense Raman spectra of pyridine at a silver electrode. *J Am Chem Soc* 99:5215–5217
25. Moscovits M (1985) Surface-enhanced spectroscopy. *Rev Mod Phys* 57:783–826
26. Nie S, Emory SR (1997) Probing single molecules and single nanoparticles by surface-enhanced Raman scattering. *Science* 275 (5303):1102–1106
27. Strekal N, Maskevich S, Maskevich A, Jardillier J-C, Nabiev I (2000) Selective enhancement of Raman or fluorescence spectra of biomolecules using specifically annealed thick gold films. *Biopolymers* 57(6):325–328
28. Gaponenko SV, Gaiduk AA, Kulakovitch OS, Maskevich SA, Strekal ND, Prokhorov OA, Shelekhina VM (2001) Raman scattering enhancement using crystallographic surface of a colloidal crystal. *JETP Lett* 74(6):309–313
29. Shadi IT, Chowdhry BZ, Snowden MJ, Withnall R (2004) Semi-quantitative analysis of alizarin and purpurin by surface-enhanced resonance Raman spectroscopy (SERRS) using silver colloids. *J Raman Spectrosc* 35(8/9):800–807
30. Stoica T, Shushunova V, Dais C, Solak H, Grutzmacher D (2007) Two-dimensional arrays of self-organized Ge islands obtained by chemical vapor deposition on pre-patterned silicon substrates. *Nanotechnology* 18:455307
31. Baranov AV, Fedorov AV, Perova TS, Moore RA, Yam V, Bouchier D, Le Thanh V, Berwick K (2006) Analysis of strain and intermixing in single-layer Ge/Si quantum dots using polarized Raman Spectroscopy. *Phys Rev B* 73:075322
32. Jin G, Tang YS, Liu JL, Wang KL (1999) Growth and study of self-organized Ge quantum wires on Si(111) substrates. *Appl Phys Lett* 74(17):2471–2473
33. Colomban P (2003) Polymerization degree and Raman identification of ancient glasses used for jewelry, ceramic enamels and mosaics. *J Non-Crystalline Solids* 323(1–3):180–187
34. Gaponenko SV (2002) Effects of photon density of states on Raman scattering in mesoscopic structures. *Phys Rev B* 65:140303(R)
35. Goulet PJG, Pieczomka NPW, Aroca RF (2003) Overtones and combinations in single-molecule surface-enhanced resonance Raman scattering spectra. *Anal Chem* 75(8):1918–1923